



Research paper

Pyrazolo[1,5-*a*]pyridine-3-carboxamide hybrids: Design, synthesis and evaluation of anti-tubercular activity



Xiaoyun Lu ^{a, b, *, 1}, Jian Tang ^{b, c, 1}, Shengyang Cui ^{b, c}, Baojie Wan ^d, Scott G. Franzblauc ^d, Tianyu Zhang ^b, Xiantao Zhang ^e, Ke Ding ^{a, b}

^a School of Pharmacy, Jinan University, 601 Huangpu Avenue West, Guangzhou, 510632, China

^b State Key Laboratory of Respiratory Diseases, Guangzhou Institutes of Biomedicine and Health, Chinese Academy of Science, #190, Kai Yuan Avenue, Guangzhou, 510530, China

^c University of Chinese Academy of Sciences, #19 Yuquan Road, Beijing, 100049, China

^d Institute for Tuberculosis Research, College of Pharmacy, University of Illinois at Chicago, 833 South Wood Street, Chicago, IL, 60612, United States

^e Guangzhou Eggbio Co., Ltd, 3 Ju Quan Road, Science Park, Guangzhou, 510663, China

ARTICLE INFO

Article history:

Received 27 June 2016

Received in revised form

8 September 2016

Accepted 9 September 2016

Available online 10 September 2016

Keywords:

Anti-tubercular

Hybrid

Mtb

Pyrazolo[1,5-*a*]pyridine-3-carboxamide

ABSTRACT

A series of pyrazolo[1,5-*a*]pyridine-3-carboxamide hybrids were designed and evaluated as novel anti-tubercular agents. The representative hybrid **7** exhibited promising *in vitro* activity against susceptible strain H37Rv and a panel of drug-resistant *Mtb* strains with MIC values of 0.006 µg/mL and ranged from 0.003 to 0.014 µg/mL, respectively. More importantly, the hybrid **7** also showed very low cytotoxicity, and could significantly reduce the mycobacterial burden in a mouse model infected with autoluminescent H37Ra strain, which may serve as a lead compound for further development of new anti-tubercular agents.

© 2016 Elsevier Masson SAS. All rights reserved.

1. Introduction

Mycobacterium tuberculosis (*Mtb*) is the causative agent of tuberculosis (TB), which remains one of the world's deadliest pandemic diseases with over 9.0 million new cases and 1.5 million deaths every year [1]. WHO recommended a standard regimen for the treatment of TB by a combination of four first-line drugs (isoniazid, rifampicin, ethambutol and pyrazinamide) with 6–9 months therapy [2]. However, multidrug-resistant (MDR), extensively drug-resistant (XDR) *Mtb* strains and comorbidity with HIV have made TB therapy difficult and ineffective. At present, MDR-TB is treated with a combination of eight to ten drugs lasting up to 18–24 months [3]. Bedaquiline (TMC207, SIRTURO[®]) was approved by FDA in 2012 as part of combination therapy for the treatment of adults with pulmonary MDR-TB [4]. However, bedaquiline prescription has to include a black-box warning due to serious adverse

effects such as the increased mortality and QT prolongation [5], which may limit its applications in clinic. Thus, there is an urgent need to develop new anti-TB drugs to shorten the treatment duration and target MDR-TB strains.

Extensive efforts were invested in the identification of novel anti-TB drugs in academic and pharmaceutical industry. Molecular hybridization of a lead scaffold and existing drugs has become a promising strategy to design and discover potent anti-TB drugs [6,7], with the purpose to enhance activity and modulate physicochemical properties. Pyrazolo[1,5-*a*]pyridine-3-carboxamide scaffold is an effective anti-TB pharmacophore published by our group (Fig. 1) [8]. The study indicated that the incorporation of lipophilic chain tail into the pyrazolo[1,5-*a*]pyridine-3-carboxamide can increase anti-TB activity and improve druggability. In view of these facts, we envisaged to design new pyrazolo[1,5-*a*]pyridine-3-carboxamide hybrids incorporated with fragment of existing clinical anti-TB drugs, which could possibly target MDR-TB strains. Several clinical representative anti-TB molecules SQ109 [9], SQ609 [10], PNU-100480 [11], PA-824 [12], TBA-354 [13] and OPC-67683 [14] (Fig. 1) share similar chain tail to that of pyrazolo[1,5-*a*]pyridine-3-carboxamide. In this study, we designed a

* Corresponding author. School of Pharmacy, Jinan University, 601 Huangpu Avenue West, Guangzhou, 510632, China.

E-mail address: luxy2016@jnu.edu.cn (X. Lu).

¹ These authors contributed equally.

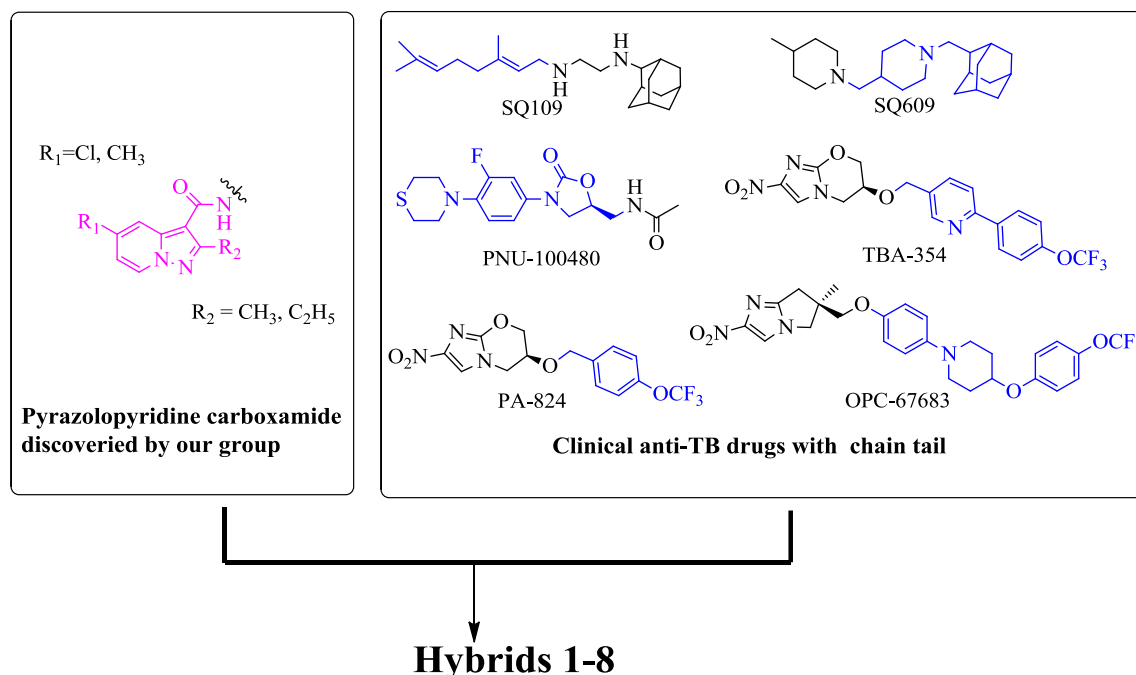


Fig. 1. Pyrazolo[1,5-*a*]pyridine-3-carboxamide core (colored in purple) and representative clinical anti-TB drugs and their tails (colored in blue). (For interpretation of the references to colour in this figure legend, the reader is referred to the web version of this article.)

new class of pyrazolo[1,5-*a*]pyridine-3-carboxamide hybrids to improve the anti-tubercular activity especially for drug resistant *Mtb* as outlined in Fig. 1.

2. Chemistry

As represented in Fig. 2, the synthetic routes of new pyrazolo[1,5-*a*]pyridine-3-carboxamide hybrids (**1–8**) involved amide bond formation between the corresponding pyrazolo[1,5-*a*]pyridine-3-carboxylic acids published by us before [8] and either commercially available or self-prepared amines. The primary amines **1a**, **3a**, and **6a** for the synthesis of compounds **1**, **3** and **6**, respectively, were commercially available. The amine **2a** was synthesized by acylation between piperidine-4-carbonitrile (**2b**) and commercially available (3*r*, 5*r*, 7*r*)-adamantane-1-carbonyl chloride (**2c**) followed by nitrile reduction with lithium aluminium hydride. Suzuki coupling of 6-chloronicotinonitrile (**5b**) or 5-chloropicolinonitrile (**7b**) and (4-(trifluoromethoxy)phen-yl)boronic acid using Pd(PPh₃)₄ and aqueous Na₂CO₃, followed by reduction with Raney Nickel, gave the amines **5a** or **7a**, respectively. The synthesis of amine **8a** was started by coupling tert-butyl 4-hydroxypiperidine-1-carboxylate (**8b**) and 4-(trifluoromethoxy)phenol (**8c**), which is followed by nucleophilic and reduction reactions based on our published procedures [8]. Finally, the title hybrids were readily obtained using a straight forward amidation of pyrazolo[1,5-*a*]pyridine-3-carboxylic acids with amines **1a–8a** in the presence of EDCI and HOBT.

3. Results and discussion

The minimum inhibitory concentration (MIC) values of all new compounds were preliminarily screened against avirulent strain H37Ra using the autoluminescent assay [15], then further determined against *M. tuberculosis* H37Rv strain using the microplate alamar blue assay (MABA) (Table 1) [16]. Isoniazid (INH) and rifampicin (RIF) were used as the positive drugs.

The first designed hybrid **1**, with an incorporation of aliphatic

tail of SQ109 to 5-chloro-2-ethylpyrazolo[1,5-*a*]pyridine core, exhibited strong antimycobacterial activity against H37Ra and H37Rv comparable to INH, with MIC values of 0.3 and 0.17 μg/mL, respectively. While incorporation of the tails of SQ609 and PNU-10048, as in compounds **2** and **3**, showed significant loss of potency in both strains. When the tail of TBA-354 was merged to the 5-chloro-2-ethylpyrazolo[1,5-*a*]pyridine core, the yielded compound **4** showed an MIC value of 0.2 μg/mL comparable to that of compound **1**. Further investigations of the substituents on the core revealed that the replacement of 5-chloro-2-ethylpyrazolo[1,5-*a*]pyridine with 2,5-dimethylpyrazolo[1,5-*a*]pyridine (**5**) could improve the antimycobacterial activity against H37Ra and H37Rv to 0.03 and 0.06 μg/mL, respectively. However, when the tail of PA-824 was merged to the 2,5-dimethylpyrazolo[1,5-*a*]pyridine, the resulted compound **6** only exhibited moderate activity. Interestingly, shifting the pyridine nitrogen of compound **5** to the ortho position (**7**) displayed a remarkable improvement of activity with MIC values of 0.003 and 0.006 μg/mL against *Mtb* strain H37Ra and H37Rv, respectively, which is more potent than INH, and comparable to RIF (Table 1). The 2,5-dimethylpyrazolo[1,5-*a*]pyridine and tail of OPC-67683 hybrid **8** was also displayed comparable MIC activity to that of RIF.

In view of their excellent potencies against *Mtb* H37Rv strain, compounds **5** and **7** were further evaluated against five drug-resistant *Mtb* isolates under aerobic conditions with INH, RIF and levofloxacin (LEV) as positive controls (Table 2) [17]. Compounds **5** and **7** also exhibited strong inhibitory activities against all five different resistant strains with MIC values ranged from 0.003 to 0.079 μg/mL, while INH, RIF and LEV showed significant activity loss against their corresponding drug-resistant strains. From the results, it was shown that compound **7** was slightly more active than compound **5**, and exhibited similar potency against both susceptible strains H37Rv and resistant isolates, suggesting its promising potential for both drug-sensitive and resistant *Mtb* strains. Moreover, compound **7** had no cytotoxicity against VERO and HepG2 cells, which displayed the IC₅₀ values of 43 μM and >100 μM,

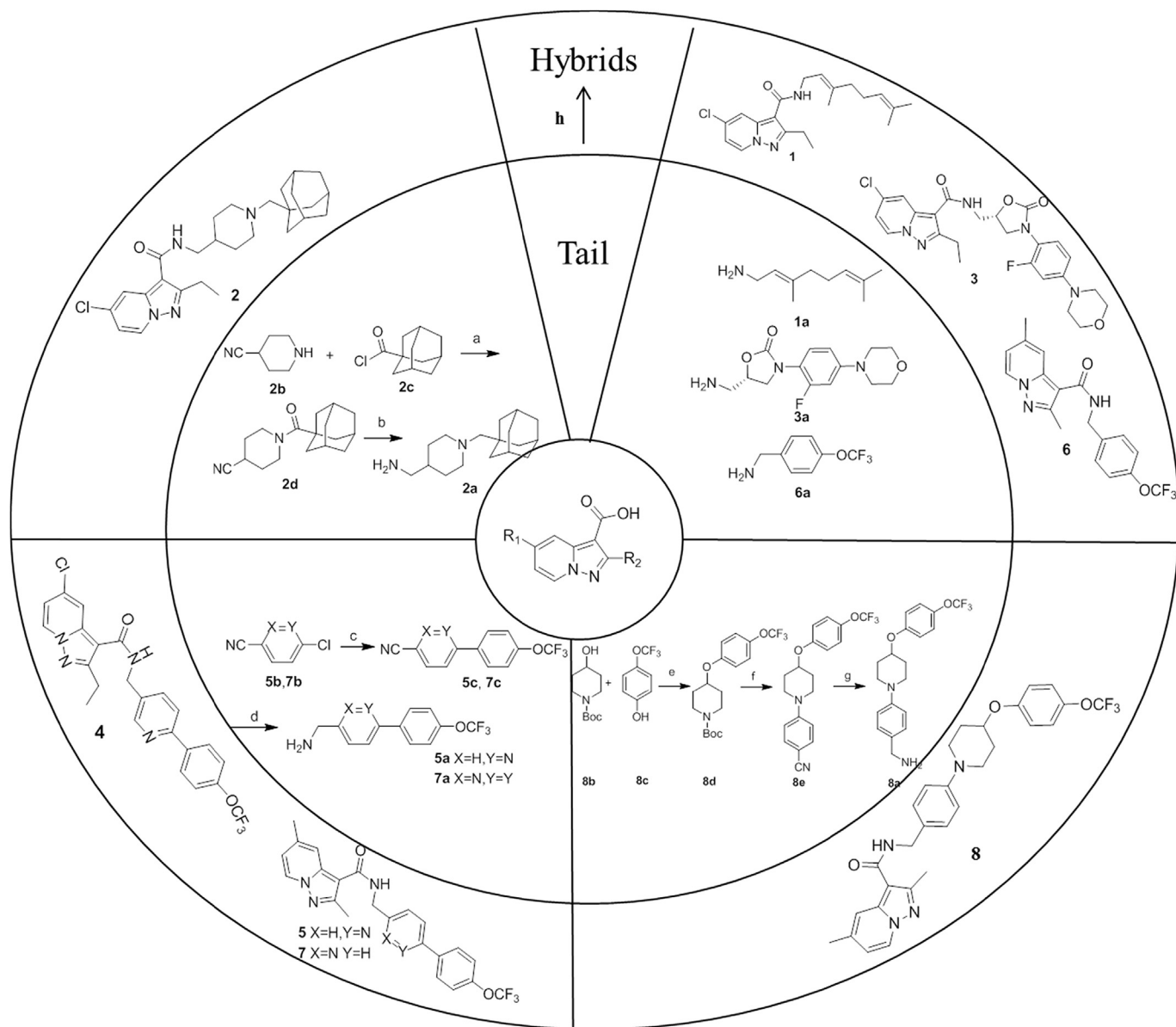


Fig. 2. Synthesis of compounds 1–8. Reagents and conditions: (a) DIPEA, DMF, r.t., 16 h, 71.0%; (b) LAH, anhydrous THF, 0 °C to reflux, overnight, 96.7%; (c) (4-(trifluoromethoxy)phenyl)boronic acid, Pd(PPh₃)₄, 2 M Na₂CO₃ (a.q.), toluene, 110 °C, overnight, 79.9%; (d) Raney Nickel, H₂, methanol, r.t., 3.5 h, 58.1%; (e) PPh₃, DEAD, THF, r.t., 18 h, 70.4%; (f) i) TFA, DCM, 0 °C to r.t., 3 h; ii) 4-florobenzonitrile, K₂CO₃, DMSO, 120 °C, 6 h, 69.2%; (g) LAH, anhydrous THF, 0 °C to r.t., 2 h, 90.6%; (h) EDCI, HOBT, Et₃N, DMF, 80 °C, overnight, 50–77%.

respectively (Table 3).

The antitubercular activity of compound 7 was further evaluated *in vivo* using a cost-efficient mouse model infected with the selectable marker-free autoluminescent *Mtb* strain H37Ra [8,18]. As shown in Fig. 3, compound 7 exhibited dose-dependent *in vivo* anti-tubercular activity. After 4-day treatment, the RLU_{dayn}/RLU_{day0} ratios were 0.96 and 0.50 for animals in the 4 and 100 mg/kg/day treated groups, respectively, while the corresponding number was about 2.68 in the untreated vehicle group. However, the RLU_{dayn}/RLU_{day0} ratios were on the rise on the day 6. The reason needs to be investigated. Nevertheless, the results suggested the promising potential of compound 7 as a lead compound for the development of new anti-TB agents.

4. Conclusions

In this paper, a series of pyrazolo[1,5-a]pyridine-3-carboxamide

hybrids incorporated with fragment of existing clinical anti-TB drugs have been designed, synthesized and evaluated for antitubercular activity. Several hybrids exhibited potent antimycobacterial activity against *Mtb* strain H37Ra and H37Rv with nanomolar MIC values, which was comparable to that of RIF. The representative hybrid 7 exhibited promising *in vitro* activities against a panel of drug-resistant *Mtb* strains with MIC values ranged from 0.003 to 0.014 μg/mL. Further *in vivo* studies indicated that compound 7 significantly reduce the mycobacterial burden in H37Ra infected mouse model, suggesting it as a new lead for further anti-tubercular drug discovery.

5. Experimental section

5.1. Chemistry

General Methods for Chemistry. All reagents and solvents were

Table 1
The *in vitro* antitubercular activity of hybrids **1–8** against the *Mtb* strains H37Rv and H37Ra.

Comps	Structure	MIC ($\mu\text{g/mL}$)	
		H37Ra ^a	H37Rv ^b
1		0.30	0.17
2		3	>1
3		>10	nd
4		0.10	0.20
5		0.03	0.06
6		3.0	0.91
7		0.003	0.006
8		0.03	0.006
INH	—	0.41	0.1
RIF	—	0.03	0.003

^a Anti-TB activity assays against H37Ra were performed using the autoluminescent assay.

^b Anti-TB activity assays against H37Rv were performed using MABA.

Table 2
Antitubercular activity of compounds **5** and **7** against drug-resistant *Mtb* strains.

Comps	MIC ($\mu\text{g/mL}$)				
	INH-R1 ^a	INH-R2 ^b	RIF-R1 ^c	RIF-R2 ^d	FQ-R1 ^e
5	0.079	0.015	0.009	0.016	0.040
7	0.014	0.006	0.003	0.006	0.009
INH	>27	>27	0.056	0.11	0.088
RIF	0.016	0.007	0.42	>41	0.017
LEV	0.44	0.59	0.37	0.63	10

^a INH-R1 (isoniazid resistant strain) was derived from H37Rv and is a *katG* mutant (Y155* = truncation).

^b INH-R2 (isoniazid resistant strain) is a strain ATCC35822.

^c RIF-R1 (rifampicin resistant strain) was derived from H37Rv and is an *rpoB* mutant (S522L).

^d RIF-R2 (rifampicin resistant strain) strain ATCC35828.

^e FQ-R1 is a fluoroquinolone-resistant strain derived from H37Rv and is a *gyrB* mutant (D94 N).

Table 3
The cytotoxicity of compound **7** against VERO and HepG2 cells.

Compd	IC ₅₀ (μM)	
	VERO ^a	HepG2 ^b
7	43	>100

^a VERO: African green monkey kidney cell line.

^b HepG2: human liver cells.

obtained from commercial sources and used without further purification. Flash chromatography was performed using silica gel (200–300 mesh). All reactions were monitored by TLC, using silica gel plates with fluorescence F₂₅₄ and UV light visualization. ¹H NMR and ¹³C NMR spectra were recorded either on a 400 MHz (¹H, 400 MHz) or 500 MHz (¹H, 500 MHz; ¹³C, 125 MHz) Bruker spectrometer. Coupling constants (*J*) are expressed in hertz (Hz). Chemical shifts (δ) of NMR are reported in parts per million (ppm) units relative to the internal residual solvent peak. The following

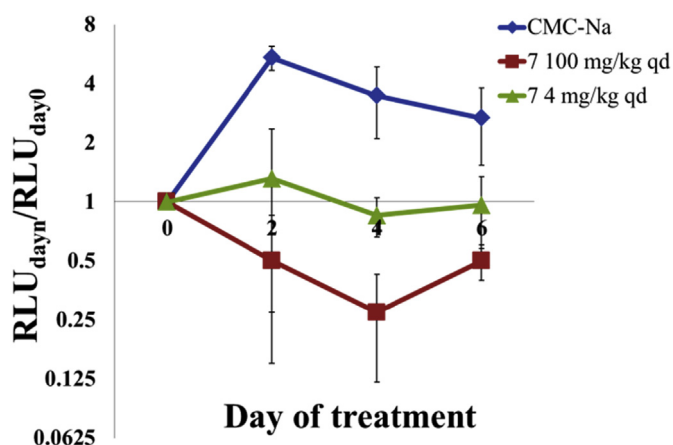


Fig. 3. Compound **7** dose-dependently inhibits the growth of *M.tb* H37Ra following 6 consecutive days of administration. Days post initial treatment (x-axis) is plotted against the corresponding RLU_{dayn}/RLU_{day0} ratio (y-axis). Blue: vehicle (CMC-Na); Red: 7 100 mg/kg qd; Green: 7 4 mg/kg qd. (For interpretation of the references to colour in this figure legend, the reader is referred to the web version of this article.)

abbreviations were used: br = broad signal, s = singlet, d = doublet, dd = doublet of doublets, t = triplet, q = quartet, m = multiplet. Low resolution ESI-MS were recorded on an Agilent 1200 HPLC-MS mass spectrometer and high resolution ESI-MS on an ABSciex TripleTOF 5600 plus System ESI-LC-MS/MS mass spectrometer. The purity of compounds was determined by reverse-phase high performance liquid chromatography (HPLC) analysis to be >95%. HPLC instrument: Dionex Summit HPLC (column: Diamonsil C18, 5.0 mm, 4.6×250 mm (Dikma Technologies); detector: PDA-100 photodiode array; pump: p-680A; injector: ASI-100 autoinjector). A flow rate of 1.0 mL/min was used with a mobile phase of MeOH in H_2O with a 0.1% ammonia.

5.1.1. (1-((3*r*, 5*r*, 7*r*)-adamantan-1-ylmethyl)piperidin-4-yl) methanamine (**2a**)

Piperidine-4-carbonitrile (**2b**, 1.00 g, 9.1 mmol) was dissolved in DMF (15 mL) and DIPEA (2, 2.94 g, 22.8 mmol) in an atmosphere of argon. (3*r*, 5*r*, 7*r*)-adamantane-1-carbonyl chloride (**2c**, 1.5 g, 7.6 mmol) dissolved in DMF (3.4 mL) was added slowly and the reaction mixture was stirred at r.t. for 16 h CH_2Cl_2 and 1 N HCl (aq) were added and the phases separated. The organic phase was evaporated to dryness and purified through flash column chromatography to afford the compound **2d** (1.48 g, 71.0%). MS (ESI) m/z 273 $[M+H]^+$.

A solution of **2d** (5.49 g, 20.0 mmol) in anhydrous THF (300 mL) was added LAH (4.6 g, 121.0 mmol) at 0 °C. After stirred for 0.5 h, the mixture was heated to reflux for overnight. The reaction was quenched with 40 mL 2 M NaOH (a.q.) and the mixture was filtered through celite and concentrated. The residue was redissolved in chloroform and washed with water. The organic layer was separated and then evaporated to dryness to afford the compound **2a** (5.07 g, 96.7%). MS (ESI) m/z 263 $[M+H]^+$.

5.1.2. (6-(4-(trifluoromethoxy)phenyl)pyridin-3-yl) methanamine (**4a** or **5a**)

A mixture solution of 6-chloronicotinonitrile (**5b**, 5.0 g, 36.1 mmol) and 2 M Na_2CO_3 (a.q. 36 mL) in toluene (100 mL) was added (4-(trifluoromethoxy)phenyl)boronic acid (11.12 g, 54.0 mmol) and $Pd(PPh_3)_4$ (0.5 g, 0.43 mmol). The mixture was evacuated and backfilled with argon (three cycles) and stirred at 110 °C for overnight. After the reaction was finished, the mixture was filtered through celite and concentrated. The residue was

purified through flash column chromatography to afford the compound **5c** (7.62 g, 79.9%) as a white solid. 1H NMR (400 MHz, $CDCl_3$) δ (ppm) 8.95 (s, 1H), 8.10 (d, $J = 8.8$ Hz, 2H), 8.03 (dd, $J = 8.4, 2.4$ Hz, 1H), 7.84 (d, $J = 8.4$ Hz, 1H), 7.36 (d, $J = 8.4$ Hz, 1H). MS (ESI) m/z 265 $[M+H]^+$.

To a stirred solution of **5c** (2.0 g, 7.57 mmol) in methanol (100 mL) was added Raney Nickel (5% e.q.). The mixture was evacuated and backfilled with hydrogen (three cycles) and stirred at room temperature for 3.5 h. After the reaction was finished, the mixture was filtered through celite and concentrated to afford the compound **5a** (1.18 g, 58.1%). 1H NMR (400 MHz, $DMSO-d_6$) δ (ppm) 8.62 (s, 1H), 8.19 (dd, $J = 8.8, 2.0$ Hz, 2H), 7.94 (d, $J = 8.0$ Hz, 1H), 7.86 (dd, $J = 8.4, 2.4$ Hz, 1H), 7.46 (d, $J = 8.4$ Hz, 2H), 3.78 (s, 2H). MS (ESI) m/z 269 $[M+H]^+$.

5.1.3. (5-(4-(trifluoromethoxy)phenyl)pyridin-2-yl) methanamine (**7a**)

Compound **7a** was prepared by the method similar to that of **5a**. 1H NMR (400 MHz, $DMSO-d_6$) δ (ppm) 8.82 (d, $J = 2.0$ Hz, 1H), 8.07 (dd, $J = 8.4, 2.4$ Hz, 2H), 7.85 (d, $J = 8.8$ Hz, 2H), 7.59 (d, $J = 8.0$ Hz, 1H), 7.48 (d, $J = 8.0$ Hz, 2H), 3.92 (s, 2H). MS (ESI) m/z 269 $[M+H]^+$.

5.1.4. (4-(4-(4-(trifluoromethoxy)phenoxy)piperidin-1-yl)phenyl) methanamine (**8a**)

To a stirred solution of 4-(trifluoromethoxy)phenol (**8c**, 1.05 g, 5.90 mmol) in THF (50 mL), 4-hydroxy-piperidine-1-carboxylic acid tert-butyl ester (**8b**, 1.08 g, 5.37 mmol) was added followed by PPh_3 (1.55 g, 5.90 mmol). The resulting reaction mixture was stirred at r.t. for 15 min. DEAD (1.20 g, 1.17 mmol) was added dropwise at 20 °C and the reaction mixture was stirred at r.t. for 18 h. After completion of the reaction, the mixture was concentrated under reduced pressure to obtain the crude material, which was further diluted with CH_2Cl_2 (50 mL). The CH_2Cl_2 layer was washed with water (3×100 mL) then dried over Na_2SO_4 , filtered and concentrated under reduced pressure to obtain the crude material, which was further purified through silica gel column chromatography to afford the compound **8d** (1.71 g, 70.4%). 1H NMR (400 MHz, $CDCl_3$) δ (ppm) 7.27 (d, $J = 8.4$ Hz, 2H), 7.07 (d, $J = 9.2$ Hz, 2H), 4.55–4.58 (m, 1H), 3.63–3.67 (m, 2H), 3.15–3.19 (m, 2H), 1.88–1.91 (m, 2H), 1.47–1.55 (m, 2H), 1.40 (s, 9H). MS (ESI) m/z 362 $[M+H]^+$.

To a solution of **8d** (1.36 g, 3.78 mmol) in anhydrous DCM (15 mL) was added trifluoroacetic acid (4.5 mL) in 0 °C and the reaction was stirred at room temperature for 3 h. After the reaction was finished, the mixture was evaporated and the residue was redissolved with EA. The solution was washed with saturated $NaHCO_3$ (a.q.) to the aqueous layer pH = 8.0. Organic layer was separated, washed with brine and evaporated to dryness, and the crude product was used without further purification.

A mixture of the resulting product and anhydrous K_2CO_3 (1.57 g, 11.34 mmol) in $DMSO$ (23 mL) was added 4-florobenzonitrile (1.14 g, 9.45 mmol). The reaction was stirred at 120 °C for 6 h. After the reaction was finished, the mixture was poured into 100 mL water with stirring and the precipitated solid was filtrated for further purification through flash column chromatography to afford the title compound **8e** (0.95 g, 69.23%). 1H NMR (400 MHz, $CDCl_3$) δ (ppm) 7.57 (d, $J = 8.4$ Hz, 2H), 7.15–7.17 (m, 4H), 6.92 (d, $J = 8.8$ Hz, 2H), 4.57 (m, 1H), 3.62–3.67 (m, 2H), 3.34–3.39 (m, 2H), 2.26 (m, 2H), 2.01 (m, 2H). MS (ESI) m/z 363 $[M+H]^+$.

A solution of **8e** (0.95 g, 2.62 mmol) in anhydrous THF (50 mL) was added LAH (0.31 g, 8.13 mmol) at 0 °C. After stirred for 0.5 h, the mixture was heated to reflux for additional 2 h. The reaction was quenched with 3 mL 2 M NaOH (a.q.) and the mixture was filtered through celite and concentrated. The residue was redissolved in EA and washed with brine. The organic layer was separated and then evaporated to dryness to afford the title compound

8a (0.87 g, 90.6%). MS (ESI) m/z 367 [M+H]⁺.

5.1.5. General procedure for synthesis of hybrids 1–8

To a stirred solution of 5-chloro-2-ethylpyrazolo[1,5-*a*]pyridine-3-carboxylic acid or 2,5-dimethylpyrazolo[1,5-*a*]pyridine-3-carboxylic acid (1.34 mmol) in DMF (20 mL) was added EDCI (0.39 g, 2.01 mmol), HOBT (91 mg, 0.67 mmol) and Et₃N (0.68 g, 6.7 mmol) at room temperature. After 1 h of stirring, **1a–8a** (1.34 mmol) was added and the reaction was heated to 80 °C for overnight. The mixture was cooled, and diluted with EA (50 mL), washed with water and brine, dried with Na₂SO₄ and concentrated. The crude product was purified by flash chromatography to afford the title compounds **1–8**.

5.1.5.1. (E)-5-chloro-N-(3,7-dimethylocta-2,6-dien-1-yl)-2-ethylpyrazolo[1,5-*a*]pyridine-3-carboxamide (1). ¹H NMR (400 MHz, DMSO-*d*₆): δ(ppm) 8.71 (d, *J* = 7.2 Hz, 1H), 7.86 (d, *J* = 2.0 Hz, 1H), 7.82 (t, *J* = 5.2 Hz, 1H), 7.00 (dd, *J* = 7.2, 2.4 Hz, 1H), 5.27 (t, *J* = 6.4 Hz, 1H), 5.09 (t, *J* = 6.8 Hz, 1H), 3.87 (t, *J* = 6.0 Hz, 2H), 2.98 (q, *J* = 7.6 Hz, 2H), 2.04–2.09 (m, 2H), 1.97–2.00 (m, 2H), 1.68 (s, 3H), 1.62 (s, 3H), 1.56 (s, 3H), 1.24 (t, *J* = 7.6 Hz, 3H). ¹³C NMR (125 MHz, CD₃Cl): δ(ppm): 163.72, 156.73, 141.96, 140.51, 133.14, 131.95, 128.95, 123.94, 120.21, 117.21, 114.30, 104.82, 39.65, 37.64, 26.57, 25.81, 22.14, 17.84, 16.51, 13.17. HRMS (ESI) calcd for C₂₀H₂₆ClN₃O [M+H]⁺: 360.1837; found 360.1836. HPLC purity = 99.24%, Rt 15.76 min.

5.1.5.2. N-((1-((3*r*,5*r*,7*r*)-adamantan-1-ylmethyl)piperidin-4-yl)methyl)-5-chloro-2-ethyl-pyrazolo[1,5-*a*]pyridine-3-carboxamide (2). ¹H NMR (400 MHz, DMSO-*d*₆): δ(ppm) 8.71 (d, *J* = 7.2 Hz, 1H), 7.84 (d, *J* = 2.0 Hz, 1H), 7.74 (t, *J* = 5.6 Hz, 1H), 7.00 (dd, *J* = 7.2, 2.0 Hz, 1H), 3.16 (t, *J* = 6.0 Hz, 2H), 2.98 (q, *J* = 7.6 Hz, 2H), 2.68–2.71 (m, 2H), 2.08–2.14 (m, 2H), 1.90 (s, 5H), 1.64–1.67 (m, 3H), 1.56–1.59 (m, 5H), 1.44–1.51 (m, 7H), 1.20–1.28 (m, 5H). ¹³C NMR (125 MHz, CD₃Cl): δ(ppm): 163.95, 156.50, 142.08, 133.18, 128.94, 118.05, 114.35, 104.88, 71.22, 56.50, 45.32, 41.11, 37.49, 36.18, 35.19, 30.79, 28.73, 22.27, 13.30. HRMS (ESI) calcd for C₂₇H₃₇ClN₄O [M+H]⁺: 469.2729; found 469.2724.

5.1.5.3. 5-chloro-2-ethyl-N-((3-(3-fluoro-4-morpholinophenyl)-2-oxooxazolidin-5-yl)methyl)pyrazolo[1,5-*a*]pyridine-3-carboxamide (3). ¹H NMR (400 MHz, DMSO-*d*₆): δ(ppm) 8.71 (d, *J* = 7.2 Hz, 1H), 8.11 (t, *J* = 5.6 Hz, 1H), 7.79 (s, 1H), 7.50–7.54 (m, 1H), 7.17–7.19 (m, 1H), 7.00–7.07 (m, 2H), 4.88–4.92 (m, 1H), 4.17 (t, *J* = 9.2 Hz, 1H), 3.86–3.90 (m, 4H), 3.71–3.73 (m, 2H), 2.92–2.95 (m, 6H), 1.19 (t, *J* = 7.2 Hz, 3H). ¹³C NMR (125 MHz, CD₃Cl): δ(ppm): 164.57, 157.26, 156.59, 154.51 (d, *J* = 30.9 Hz, 1C), 142.03, 136.66 (d, *J* = 9.0 Hz, 1C), 133.77, 133.05 (d, *J* = 10.5 Hz, 1C), 129.15, 118.95 (d, *J* = 4.2 Hz, 1C), 117.62, 114.56, 114.02 (d, *J* = 3.2 Hz, 1C), 107.61 (d, *J* = 26.2 Hz, 1C), 103.80, 67.19, 67.07, 51.11 (d, *J* = 2.8 Hz, 1C), 47.91, 42.10, 22.19, 13.00. HRMS (ESI) calcd for C₂₄H₂₅ClFN₅O₄ [M+H]⁺: 502.1652; found 502.1648. HPLC purity = 99.85%, Rt 5.80 min.

5.1.5.4. 5-chloro-2-ethyl-N-((6-(4-(trifluoromethoxy)phenyl)pyridin-3-yl)methyl)pyrazolo[1,5-*a*]pyridine-3-carboxamide (4). ¹H NMR (400 MHz, DMSO-*d*₆): δ(ppm) 8.74 (d, *J* = 7.6 Hz, 1H), 8.68 (s, 1H), 8.32 (t, *J* = 5.6 Hz, 1H), 8.20 (d, *J* = 8.8 Hz, 2H), 7.96–8.00 (m, 2H), 7.88 (dd, *J* = 8.0, 1.6 Hz, 1H), 7.47 (d, *J* = 8.4 Hz, 2H), 7.04 (dd, *J* = 7.2, 2.0 Hz, 1H), 4.55 (d, *J* = 6.0 Hz, 2H), 3.02 (q, *J* = 7.2 Hz, 2H), 1.25 (t, *J* = 7.6 Hz, 3H). ¹³C NMR (125 MHz, CDCl₃): δ(ppm): 164.03, 156.84, 155.58, 150.09, 149.25, 142.24, 137.75, 136.70, 133.70, 133.19, 129.11, 128.50, 121.23, 120.65 (q, *J* = 25.6 Hz, 1C), 120.52, 117.93, 114.61, 104.14, 41.02, 22.36, 13.12. HRMS (ESI) calcd for C₂₃H₁₈F₃N₄O₂ [M+H]⁺: 475.1143; found 475.1138. HPLC purity = 98.03%, Rt 6.11 min.

5.1.5.5. 2,5-dimethyl-N-((5-(4-(trifluoromethoxy)phenyl)pyridin-2-yl)methyl)pyrazolo[1,5-*a*]pyridine-3-carboxamide (5). ¹H NMR (400 MHz, DMSO-*d*₆): δ(ppm) 8.86 (s, 1H), 8.55 (d, *J* = 7.2 Hz, 1H), 8.09 (m, 2H), 7.86 (d, *J* = 8.8 Hz, 2H), 7.80 (s, 1H), 7.48 (m, 3H), 6.83 (dd, *J* = 7.2, 1.6 Hz, 1H), 4.64 (d, *J* = 6.0 Hz, 2H), 2.59 (s, 3H), 2.39 (s, 3H). ¹³C NMR (125 MHz, CDCl₃): δ(ppm): 164.59, 156.22, 151.26, 149.43, 147.47, 142.19, 137.75, 136.45, 135.36, 134.28, 128.66, 127.60, 122.24, 121.72, 120.62 (q, *J* = 25.6 Hz, 1C), 117.57, 115.54, 103.87, 44.31, 21.58, 14.93. HRMS (ESI) calcd for C₂₃H₁₉F₃N₄O₂ [M+H]⁺: 441.1533; found 441.1530. HPLC purity = 99.50%, Rt 5.67 min.

5.1.5.6. 2,5-dimethyl-N-(4-(trifluoromethoxy)benzyl)pyrazolo[1,5-*a*]pyridine-3-carboxamide (6). ¹H NMR (400 MHz, DMSO-*d*₆): δ(ppm) 8.53 (d, *J* = 7.2 Hz, 1H), 8.04 (t, *J* = 5.6 Hz, 1H), 7.73 (s, 1H), 7.47 (d, *J* = 8.8 Hz, 2H), 7.33 (d, *J* = 8.0 Hz, 2H), 6.81 (dd, *J* = 7.2, 1.6 Hz, 1H), 4.50, 2.55 (s, 3H), 2.38 (s, 3H). ¹³C NMR (125 MHz, CDCl₃): δ(ppm): 164.54, 150.63, 148.63, 142.24, 137.90, 129.10, 127.61, 121.39, 120.61 (q, *J* = 25.6 Hz, 1C), 117.459, 115.692, 103.58, 42.82, 21.51, 14.89. HRMS (ESI) calcd for C₁₈H₁₆F₃N₃O₂ [M+H]⁺: 364.1267; found 364.1270. HPLC purity = 99.77%, Rt 6.48 min.

5.1.5.7. 2,5-dimethyl-N-((6-(4-(trifluoromethoxy)phenyl)pyridin-3-yl)methyl)pyrazolo[1,5-*a*]pyridine-3-carboxamide (7). ¹H NMR (400 MHz, DMSO-*d*₆): δ(ppm) 8.68 (s, 1H), 8.53 (d, *J* = 6.8 Hz, 1H), 8.20 (d, *J* = 8.8 Hz, 2H), 8.08 (t, *J* = 5.8 Hz, 1H), 7.98 (d, *J* = 8.4 Hz, 2H), 7.88 (dd, *J* = 8.2, 2.2 Hz, 1H), 7.74 (s, 1H), 7.47 (d, *J* = 8.0 Hz, 2H), 6.82 (dd, *J* = 7.2, 1.6 Hz, 1H), 4.55 (d, *J* = 5.6 Hz, 2H), 2.56 (s, 3H), 2.39 (s, 3H). ¹³C NMR (125 MHz, CDCl₃): δ(ppm): 164.65, 155.40, 150.69, 150.02, 150.01, 149.20, 142.22, 138.09, 137.78, 136.64, 133.49, 128.45, 127.64, 121.19, 120.61 (q, *J* = 25.6 Hz, 1C), 117.40, 115.76, 103.44, 40.86, 21.54, 14.92. HRMS (ESI) calcd for C₂₃H₁₉F₃N₄O₂ [M+H]⁺: 441.1533; found 441.1530. HPLC purity = 98.41%, Rt 5.24 min.

5.1.5.8. 2,5-dimethyl-N-(4-(4-(4-(trifluoromethoxy)phenoxy)piperidin-1-yl)benzyl)pyrazolo[1,5-*a*]pyridine-3-carboxamide (8). ¹H NMR (400 MHz, DMSO-*d*₆): δ(ppm) 8.51 (d, *J* = 8.0 Hz, 1H), 7.90 (t, *J* = 6.0 Hz, 1H), 7.70 (s, 1H), 7.27 (d, *J* = 8.4 Hz, 2H), 7.21 (d, *J* = 8.4 Hz, 2H), 7.07 (d, *J* = 9.2 Hz, 2H), 6.93 (d, *J* = 8.8 Hz, 2H), 6.80 (d, *J* = 7.2 Hz, 1H), 4.55–4.59 (m, 1H), 4.38 (d, *J* = 6.0 Hz, 2H), 3.47–3.50 (m, 2H), 2.99–3.04 (m, 2H), 2.53 (s, 3H), 2.37 (s, 3H), 2.02–2.04 (m, 2H), 1.68–1.74 (m, 2H). ¹³C NMR (125 MHz, CDCl₃): δ(ppm): 164.41, 156.00, 150.80, 150.60, 143.00, 142.99, 142.15, 137.66, 129.75, 128.93, 127.55, 122.62, 120.72 (q, *J* = 25.5 Hz, 1C), 117.51, 117.03, 116.86, 115.56, 103.93, 73.04, 46.80, 43.19, 30.53, 21.53, 14.82. HRMS (ESI) calcd for C₂₉H₂₉F₃N₄O₃ [M+H]⁺: 539.2264; found 539.2261. HPLC purity = 97.85%, Rt 7.15 min.

5.2. Biological assay

5.2.1. In vitro anti-tubercular activity using a selectable marker-free autoluminescent assay against *Mtb* H37Ra.

UAIra (*Mtb* H37Ra:pTYOK) was homogenized with sterile glass beads in a 50 mL tube containing 5 mL Middlebrook 7H9 medium plus 0.05% Tween 80, 10% v/v oleic acid albumin dextrose catalase (OADC) supplement (7H9-OADC-Tw). When OD₆₀₀ reached 0.3–0.5, relative light unit (RLU) count was determined. by putting 200 μL culture on the detection hole of the luminometer. When the RLU reached 2 million, the effect concentration of compounds **1–8** was assessed over a range of 3-fold increasing from 0.000001 μg/mL to 10 μg/mL prepared in 25 μL UAIra broth culture (RLU diluted to 2000–4000) grown in 7H9 broth with Tween80. In the treatment group, DMSO was used as negative control and isoniazide (INH, 10 μg/mL, 1 μg/mL and 0.1 μg/mL) and rifampicin (RIF, 10 μg/mL, 1 μg/mL and 0.1 μg/mL) were used as positive control. RLU counts were determined daily, for 4 days. Analysis of the data, the

MIC_{lux} value is the lowest drug concentration that can achieve the ratio (RLU_{drug}/RLU_{DMSO}) less than 10% after treatment.

5.2.2. *In vitro* anti-tubercular activity using the microplate alamar blue assay (MABA) against *M.tb* H37Rv

The test compound MICs against TB were assessed by the MABA using isoniazid and RIF (supplied by University of Illinois) as positive controls. The stock solutions of compounds were prepared in DMSO at a concentration of 5 mg/mL or 2 mg/mL, and the final test concentrations ranged from 0.05 to 5 µg/mL or from 0.004 to 1 µg/mL. Two-fold dilutions of compounds were prepared in Middlebrook 7H12 medium (7H9 broth containing 0.1% w/v casitone, 5.6 µg/mL palmitic acid, 5 mg/mL bovine serum albumin, 4 mg/mL catalase, filter-sterilized) in a volume of 100 µL in 96-well microplates (black viewplates). *M. tuberculosis* H37Rv (100 µL inoculum of 2×10^5 cfu/mL) was added, yielding a final testing volume of 200 µL. The plates were incubated at 37 °C. On the 7th day of incubation 12.5 µL of 20% Tween 80 and 20 µL of Alamar Blue (Trek Diagnostic, Westlake, OH) were added to the test plate. After incubation at 37 °C for 16–24 h, fluorescence of the wells was measured (ex 530, em 590 nm). The MICs were interpolated values obtained by using an in-house curve-fitting program and defined as the lowest concentration affecting a reduction in fluorescence of $\geq 90\%$ relative to the mean of replicate bacteria-only controls.

5.2.3. MIC values of compounds against single drugs resistant strains

The MIC of compound was determined by measuring bacterial growth after 5 d in the presence of test compounds. Compounds were prepared as 10-point two-fold serial dilutions in DMSO and diluted into 7H9-Tw-OADC medium in 96-well plates with a final DMSO concentration of 2%. The highest concentration of compound was 200 µM where compounds were soluble in DMSO at 10 mM. Each plate included assay controls for background (medium/DMSO only, no bacterial cells), zero growth (100 µM rifampicin) and maximum growth (DMSO only), as well as a rifampicin dose response curve. Plates were inoculated with *M. tuberculosis* and incubated for 5 days; growth was measured by OD₅₉₀. To calculate the MIC, the 10-point dose response curve was plotted as % growth and fitted to the Gompertz model using GraphPad Prism 5. The MIC was defined as the minimum concentration at which growth was completely inhibited and was calculated from the inflection point of the fitted curve to the lower asymptote (zero growth). In addition dose response curves were generated using the Levenberg-Marquardt algorithm and the concentrations that resulted in 50% and 90% inhibition of growth were determined (IC₅₀ and IC₉₀ respectively).

MIC values were reported when the following quality control criteria were satisfied:

- For each plate
 - No growth in the background (un-inoculated) control wells
 - OD₅₉₀ > 0.2 in maximum growth wells
 - Rifampicin MIC within 3-fold of the expected value
- For each compound curve. MIC values were reported if
 - There were 2 points with growth >75%
 - There were 2 points with growth <75%
- If no point reached 75% inhibition, the MIC was reported as > maximum concentration tested.

5.2.4. VERO cytotoxicity assay

Vero cells (ATCC CRL-1586) were maintained in RPMI-1640 with 5% FBS and 1% PS. Cells of log phase were used. 500 cells/well were seeded in 384-PP plates with a 50 µL volume. Compounds were

dissolved to 10 mM with DMSO, and a 3-fold serial dilution of the compounds from 100 µM to 0.003 µM was performed. 500 nL of compound solution was correspondingly added using Echo520 to the 384-PP plate and 500 nL DMSO instead of compound solution was used as the 0% inhibitor control. After coincubation for 72 h, 3 µL CCK8 (5 mg/mL) was added. 2 h later at 37 °C, the plates were read in the Envision Multilabel Reader at 450 nm. Cell survival rate (activity%) was calculated with the formula: activity% = (OD_{experiment} - OD_{blank}) / (OD_{control} - OD_{blank}) * 100. The resulted data was then analyzed with corresponding compound concentrations using GraphPad Prism 5 Demo. The IC₅₀ were fitted using a nonlinear regression model with a sigmoidal dose response.

5.2.5. HepG2 cytotoxicity assay

The cytotoxicity of compounds was determined by measuring HepG2 cell viability growth after 3 d in the presence of test compounds. Compounds were prepared as 10-point three-fold serial dilutions in DMSO. The highest concentration of compound tested was 100 µM where compounds were soluble in DMSO at 10 mM. HepG2 cells were cultured in complete DMEM, inoculated into 384-well assay plates containing compounds and incubated for 24 h at 37 °C, 5% CO₂. Compounds were added and cells were cultured for a further 72 h. The final DMSO concentration was 1%. Cell viability was determined using the CellTiter-Glo[®] Luminescent Cell Viability Assay (Promega) and measuring relative luminescent units (RLU). The dose response curve was fitted using the Levenberg-Marquardt algorithm. The TC₅₀ was defined as the compound concentration that produced 50% loss of cell viability. Each run included staurosporine as a control.

5.2.6. *In vivo* anti-tubercular activity of compound 7

UAIra (*M.tb* H37Ra:pTYOK) isolated on plates were homogenized with sterile glass beads in a 250 mL flask containing 50 mL 7H9 with Tween80. When RLU reached 2 million/ml, the culture were used to infect 4-to-6-week-old male BALB/c mice by tail vein injection. The day after infection (day 0), RLU counts were determined. The mice were first anesthetized by isoflurane inhalation and the RLU count was determined by laying the breast of mouse on the detection hole of the luminometer and measuring light production for 3 s for twice. Mice with similar RLU readings were randomly allocated to treatment groups (4 mice/group) and individually marked. The treatment groups received: CMC-Na alone as negative control, **7** (100 mg/kg) and **7** (4 mg/kg). Treatment was administrated daily, while RLU were detected on day 2, day 4, day 6.

Acknowledgments

We thank Guangdong Special Branch Program Technology Young talents (2014TQ01R341) and Guangdong Natural Science Funds (2016A030313106) for the financial support. In addition, this work was supported by National Institutes of Health and the National Institute of Allergy and Infectious Diseases, Contract No. HHSN272201100009I.

Appendix A. Supplementary data

Supplementary data related to this article can be found at <http://dx.doi.org/10.1016/j.ejmech.2016.09.030>.

References

- [1] WHO. Global Tuberculosis Report 2015. http://www.who.int/tb/publications/global_report/en/.
- [2] World Health Organization Treatment of Tuberculosis, Guidelines for National Programmes WHO/HTM/TB/2009.420, fourth ed., 2009. English.
- [3] World Health Organization, Guidelines for the Programmatic Management of

- Drug-resistant Tuberculosis: Emergency Update 2008 (WHO/HTM/TB/2008.402), World Health Organization, Geneva, Switzerland, 2008.
- [4] J. Cohen, Infectious disease. Approval of novel TB drug celebrated—with restraint, *Science* 339 (2013) 130.
- [5] A.H. Diacon, A. Pym, M.P. Grobusch, J.M. de los Rios, E. Gotuzzo, I. Vasilyeva, V. Leimane, K. Andries, N. Bakare, T. De Marez, M. Haxaire-Theeuwes, N. Lounis, P. Meyvisch, E. De Paepe, R.P.G. van Heeswijk, B. Dannemann, Multidrug-resistant tuberculosis and culture conversion with bedaquiline, *N. Engl. J. Med.* 371 (2014) 723–732.
- [6] N. Nayak, J. Ramprasad, U. Dalimba, New INH-pyrazole analogs: design, synthesis and evaluation of antitubercular and antibacterial activity, *Bioorg. Med. Chem. Lett.* 25 (2015) 5540–5545.
- [7] D.F. Rakesh, M.S. Bruhn, A.P. Scherman, L. Singh, J. Yang, A.J. Liu, R.E. Lenaerts, Lee, synthesis and evaluation of pretomanid (PA-824) oxazolidinone hybrids, *Bioorg. Med. Chem. Lett.* 26 (2016) 388–391.
- [8] J. Tang, B.X. Wang, T. Wu, J.T. Wan, Z.C. Tu, M. Njire, B.J. Wan, S.G. Franzblau, T.Y. Zhang, X.Y. Lu, K. Ding, Design, Synthesis, and Biological Evaluation of Pyrazolo[1,5-a]pyridine-3-carboxamides as Novel Antitubercular Agents, *ACS Med. Chem. Lett.* 6 (2015) 814–818.
- [9] O.K. Onajole, Y. Coovadia, H.G. Kruger, G.E. Maguire, M. Pillay, T. Govender, Novel polycyclic 'cage'-1,2-diamines as potential anti-tuberculosis agents, *Eur. J. Med. Chem.* 54 (2012) 1–9.
- [10] E. Bogatcheva, C. Hanrahan, B. Nikonenko, G. de los Santos, V. Reddy, P. Chen, F. Barbosa, L. Einck, C. Nacy, M. Protopopova, Identification of SQ609 as a lead compound from a library of dipiperidines, *Bioorg. Med. Chem. Lett.* 21 (2011) 5353–5357.
- [11] M. Zhang, C. Sala, N. Dhar, A. Vocat, V.K. Sambandamurthy, S. Sharma, G. Marriner, V. Balasubramanian, S.T. Cole, In vitro and in vivo activities of three oxazolidinones against nonreplicating *Mycobacterium tuberculosis*, *Antimicrob. Agents Chemother.* 58 (2014) 3217–3223.
- [12] A.M. Thompson, H.S. Sutherland, B.D. Palmer, I. Kmentova, A. Blaser, S.G. Franzblau, B. Wan, Y. Wang, Z. Ma, W.A. Denny, Synthesis and structure-activity relationships of varied ether linker analogues of the antitubercular drug (6S)-2-nitro-6-([4-(trifluoromethoxy)benzyl]oxy)-6,7-dihydro-5h-imidazo[2,1-b][1,3]oxazine(PA-824), *J. Med. Chem.* 54 (2011) 6563–6585.
- [13] A.M. Upton, S. Cho, T.J. Yang, Y. Kim, Y. Wang, Y. Lu, B. Wang, J. Xu, K. Mdluli, Z. Ma, S.G. Franzblau, In vitro and in vivo activities of the nitroimidazole TBA-354 against *Mycobacterium tuberculosis*, *Antimicrob. Agents Chemother.* 59 (2015) 136–144.
- [14] K. Stinson, N. Kurepina, A. Venter, M. Fujiwara, M. Kawasaki, J. Timm, E. Shashkina, B.N. Kreiswirth, Y. Liu, M. Matsumoto, L. Geiter, MIC of Delamanid (OPC-67683) against *Mycobacterium tuberculosis* Clinical Isolates and a Proposed Critical Concentration, *Antimicrob. Agents Chemother.* 60 (2016) 3316–3322.
- [15] T. Zhang, S.Y. Li, E.L. Nuermberger, Autoluminescent *Mycobacterium tuberculosis* for rapid, real-time, non-invasive assessment of drug and vaccine efficacy, *PLoS One* 7 (2012) e29774.
- [16] L. Collins, S.G. Franzblau, Microplate alamar blue assay versus BACTEC 460 system for high-throughput screening of compounds against *Mycobacterium tuberculosis* and *Mycobacterium avium*, *Antimicrob. Agents Chemother.* 41 (1997) 1004–1009.
- [17] J. Ollinger, M.A. Bailey, G.C. Moraski, A. Casey, S. Florio, T. Alling, M.J. Miller, T. Parish, A dual read-out assay to evaluate the potency of compounds active against *Mycobacterium tuberculosis*, *PLoS One* 8 (2013) e6053.
- [18] T.Y. Zhang, S.Y. Li, E.L. Nuermberger, Autoluminescent *Mycobacterium tuberculosis* for rapid, real-time, non-invasive assessment of drug and vaccine efficacy, *PLoS One* 7 (2012) e29774.